

Large scale bias and stochasticity of halos and dark matter

Uroš Seljak ¹ & Michael S. Warren ²

¹ Department of Physics, Jadwin Hall

Princeton University, Princeton, NJ 08544

² Theoretical Astrophysics (T-6), Mail Stop B227, Los Alamos National Laboratory, Los Alamos, NM 87545

14 December 2018

ABSTRACT

On large scales galaxies and their halos are usually assumed to trace the dark matter with a constant bias and dark matter is assumed to trace the linear density field. We test these assumption using several large N-body simulations with 384^3 – 768^3 particles and box sizes of 96 – $1152h^{-1}\text{Mpc}$, which can both resolve the small galactic size halos and sample the large scale fluctuations. We explore the average halo bias relation as a function of halo mass and show that existing fitting formulae overestimate the halo bias by up to 20% in the regime just below the nonlinear mass. We propose a new expression that fits our simulations well. We find that the halo bias is nearly constant, $b \sim 0.65$ – 0.7 , for masses below one tenth of the nonlinear mass. We explore next the relation between the initial and final dark matter in individual Fourier modes and show that there are significant fluctuations in their ratio, ranging from 10% rms at $k \sim 0.03h/\text{Mpc}$ to 50% rms at $k \sim 0.1h/\text{Mpc}$. We argue that these large fluctuations are caused by perturbative effects beyond the linear theory, which are dominated by long wavelength modes with large random fluctuations. Similar or larger fluctuations exist between halos and dark matter and between halos of different mass. While these fluctuations are small compared to the sampling variance, they are significant for attempts to determine the bias by relating directly the maps of galaxies and dark matter or the maps of different galaxy populations, which would otherwise be immune to sampling variance.

1 INTRODUCTION

Determination of the power spectrum of mass fluctuations and its redshift evolution is one of the main goals of modern observational cosmology. Its accurate measurement would allow us to test some of the most fundamental questions in cosmology today, such as the shape of primordial power spectrum and its relation to fundamental theories of structure formation, the mass of neutrino and the nature of dark energy.

In general there are two approaches to the measurement of the matter power spectrum. One is to measure galaxies, either in redshift space or in angular position (perhaps supplemented by photometric redshift information) and to assume they trace the dark matter. This assumption is believed to be valid on large scales, where the so called linear bias model assumes that the galaxy density field is proportional to the matter density field times a free parameter called bias. While power spectrum measurements of galaxies with modern surveys such as SDSS (Tegmark et al. 2003) or 2dF(Percival et al. 2002) have enormous statistical power, they can only determine the shape of the matter power spectrum and not its amplitude because of the bias uncertainties. This limits their use in the study of the growth factor evolution, important for investigations of dark energy models. In addition, on small scales information from galaxy clustering is limited by the uncertainties in the relation between

the galaxies and the dark matter, which make the bias scale dependent. For this reason the small scale information is usually discarded.

The situation with galaxies would not be as hopeless if we could determine the bias. Here we propose and explore a method to determine galaxy bias based on determination of clustering amplitude of faint galaxies. These are likely to occupy low mass halos which, as we show in this paper, have a well determined large scale bias that is independent of halo mass. Thus, measuring the large scale power spectrum amplitude for these galaxies immediately determines the matter power spectrum amplitude as well. The main problem is that in a typical flux limited survey faint galaxies occupy a small nearby volume, so the sampling variance errors for power spectrum on large scales are large. However, we can still determine their bias relative to a population of brighter galaxies. If there is no stochasticity between the two populations then a direct comparison of the maps gives an accurate determination of the relative bias with no sampling variance. We can then use the power spectrum determination of the brighter population, with smaller sampling variance errors because of larger volume covered, to determine the power spectrum of the fainter population and of the matter itself.

Another approach to determine matter fluctuations is to use weak lensing induced correlations between background galaxy ellipticities. These are sensitive to the dark matter

fluctuations directly and as such this approach holds the promise to improve upon the limitations of the galaxy clustering methods. Its main limitation is that it traces the dark matter in angular projection and has large sampling variance errors on large scales. This limits the statistical power of the weak lensing surveys. On small scales the nonlinear corrections, noise, intrinsic correlations and other systematic contaminations become significant, all of which may complicate the modelling.

A possible approach to achieve the best of both worlds is to combine the weak lensing and galaxy clustering surveys: one can use the weak lensing to determine the galaxy bias and then use the 3-d galaxy clustering information to improve on the statistical errors. One way to do this is to use galaxy-dark matter cross-correlation analysis from weak lensing and combine it with the galaxy auto-correlation analysis. If galaxies are tracing perfectly the dark matter then it suffices to have a few well measured modes in both fields to determine the galaxy bias. This has been proposed as a way to get around the sampling variance in weak lensing surveys (Pen 2004). In the absence of stochasticity it gives the bias (and so the dark matter power spectrum) without the usual sampling variance errors, assuming the analysis is done on the same patch of the sky and with the correct radial weighting of the galaxies to match that of the dark matter.

In both of these cases the underlying assumption is that there is no stochasticity between these fields on large scales. While there have been analytic attempts to address this assumption (Matsubara 1999), with simulations it has not been tested well in the past due to the lack of sufficient dynamic range. One must resolve the halos small enough to be suitable as galaxy hosts (with typical masses at or below $10^{12}h^{-1}M_{\odot}$). At the same time, the simulations must be large enough so that many long wavelength modes are sampled to determine the statistics of interest. We achieve this by using a set of new simulations with a larger dynamical range. The number of particles in these simulations, $10^8 - 10^9$, and their box size, $100-1000h^{-1}\text{Mpc}$, allow a much better exploration of the halo bias and stochasticity on larger scales than available before.

In addition to exploring the relation between halos and matter we can also investigate the relation between the initial and final matter distribution. Weak lensing measures the nonlinear matter field, while for the study of linear growth factor one would like to know the relation between galaxies and linear matter field instead. We explore the relation between the final and initial dark matter density field on large scales, where this relation is believed to be perfect. This case is amenable to perturbation theory analysis and as such allows one to interpret and verify the numerical simulation results.

Finally, we revisit the question of halo bias as a function of halo mass with the new simulations. This has been addressed by previous generation of simulations using 256^3 particles and box sizes of order $(100-140)h^{-1}\text{Mpc}$ (Jing 1998; Sheth & Tormen 1999; Sheth et al. 2001). This, as noted by the authors themselves, is barely adequate for this purpose because of large shot noise at high halo masses and insufficient number of large scale modes where linear evolution is valid. The goal of these papers was to provide expressions which fit over a range of power law simulations and were

not specifically optimized for realistic ΛCDM models. They provide expressions that fit the simulations available at the time to a reasonable accuracy, but which can be systematically wrong by as much as 10-20%. To put things into a current context, the statistical error on the amplitude of galaxy clustering from SDSS using $k < 0.2h/\text{Mpc}$ modes is 1% (Tegmark et al. 2003), so a perfect bias determination, for example using the faint galaxies as described above, would allow us to reach this accuracy on the matter power spectrum.

2 SIMULATIONS

The N-body code we use in this paper is the Hashed Oct-tree code (HOT), a parallel, tree based, code (Warren & Salmon 1993). This code was compared to a variety of other simulation codes in Frenk et al. (1999), and further validation studies will be presented elsewhere. For this paper we performed several simulations with this code. The smallest was a $96h^{-1}\text{Mpc}$ box size, 512^3 particle run (HOT1). This simulation has a particle mass of $5.5 \times 10^8h^{-1}M_{\odot}$ and is useful for probing the halo bias at the low mass end, below $10^{11}h^{-1}M_{\odot}$. It suffers from the small box size which makes the investigations on linear scales difficult and makes the shot noise fluctuations for higher mass halos (with lower halo numbers) very large. Next up in size is a simulation with $288h^{-1}\text{Mpc}$ box and 768^3 particles (HOT2). This is the main simulation that we use in this paper, as it has an optimal combination of box size and particle mass for our purposes. It samples the Fourier modes down to $k \sim 0.02h/\text{Mpc}$ and has many modes at $k \sim 0.1h/\text{Mpc}$, where the power spectrum is still close to linear. This is also the typical scale probed by the current surveys such as SDSS and 2dF. The particle mass for this simulation is $4.4 \times 10^9h^{-1}M_{\odot}$ and can resolve halos down to a few times $10^{11}h^{-1}M_{\odot}$, which is sufficient for typical galaxies in a flux limited sample. Finally, for determination of the halo bias at the high mass end we use a simulation with $1152h^{-1}\text{Mpc}$ box size and 768^3 particles (HOT3). This simulation has large enough box to sample long wavelength modes well, but its particle mass of $2.8 \times 10^{11}h^{-1}M_{\odot}$ does not allow us to resolve galactic size halos and we limit its use to group and cluster size halos.

The tree-code accuracy was controlled using the absolute error criterion described in Salmon & Warren (1994), which ranged from $10^{-5}M_{\text{tot}}/R_0^2$ per interaction at the start of the each simulation, to $10^{-3}M_{\text{tot}}/R_0^2$ at the end. Plummer smoothing was used, with softening lengths of 7, 20 and 95 comoving kpc for models 1, 2 and 3 respectively. The number of timesteps for model 1 was 1475, 736 for model 2, and 725 for model 3. Model 1 started at a redshift of 50, model 2 at 44, and model 3 at 27. All particle masses were identical, with the initial particle displacements imposed on a cubical lattice.

All of these simulations are normalized to $\sigma_8 = 0.9$ and have $\Omega_m = 0.3$, $\Omega_b = 0.04$ and Hubble parameter $h = 0.7$. They use realistic transfer functions from CMBFAST (Seljak & Zaldarriaga 1996). $\sigma_8 = 0.9$ corresponds to $\delta_\zeta = 4.624 \times 10^{-5}$ normalization in CMBFAST. In the following all the results are for HOT2 whenever not explicitly specified otherwise.

For the purpose of studying bias as a function of halo

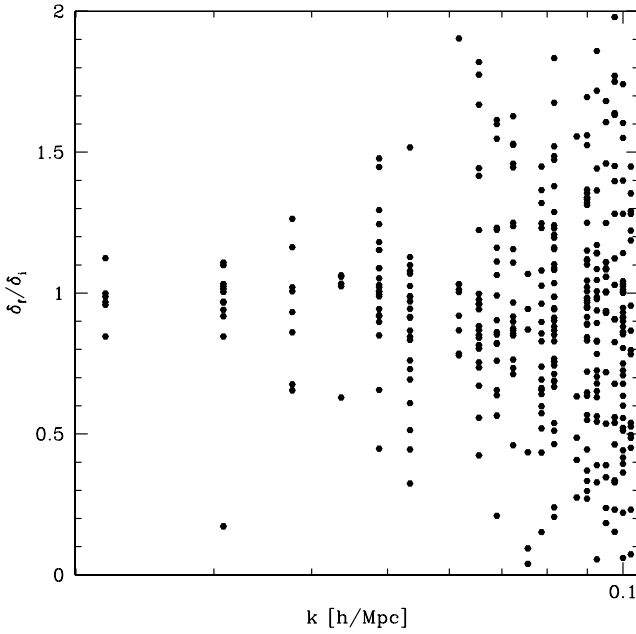


Figure 1. Ratio of final to initial density perturbations as a function of wavemode amplitude k . There is a large scatter between the two quantities even on large scales, where linear theory is usually assumed to be valid.

mass we also ran a suite of simulations varying one parameter at a time. The box size for these simulations is $192h^{-1}\text{Mpc}$ with 512^3 particles. Their force and mass resolution is the same as for HOT2. We ran the basic simulation with the same parameters as for HOT1-3, as well as $\Omega_m = 0.2$, $\sigma_8 = 0.8$, $n = 0.9$, $dn/d\ln k = -0.04$ and $h = 0.6$, 6 simulations in total. We used the same seed in random generator for all of these cases to minimize the sampling errors. To investigate the bias at low mass end we supplemented these simulations with another run with 512^3 particles in $96h^{-1}\text{Mpc}$.

Finally, to investigate the bias at the high mass end we used additional simulations with 384^3 particles in $768h^{-1}\text{Mpc}$ box, with standard parameters and $\sigma_8 = 0.775$ and $\sigma_8 = 1.046$. We also used another simulation with $700h^{-1}\text{Mpc}$ and 512^3 box for which $\sigma_8 = 0.767$, $\Omega_m = 0.27$ and $h = 0.71$.

3 STOCHASTICITY OF DARK MATTER

We begin by exploring the relation between the final dark matter density field and the initial density field, rescaled to $z = 0$ using the linear growth factor. We Fourier transform both fields and denote individual modes with $\delta_i(\mathbf{k})$ and $\delta_f(\mathbf{k})$ (we treat real and imaginary components as separate modes). Figure 1 shows the ratio $b(\mathbf{k}) = \delta_f(\mathbf{k})/\delta_i(\mathbf{k})$ for $k < 0.1h/\text{Mpc}$. This is the scale at which one often assumes linear theory to be valid. We see that there are significant fluctuations between the initial and final field, suggesting that there are large corrections to the linear evolution even for $k < 0.1h/\text{Mpc}$.

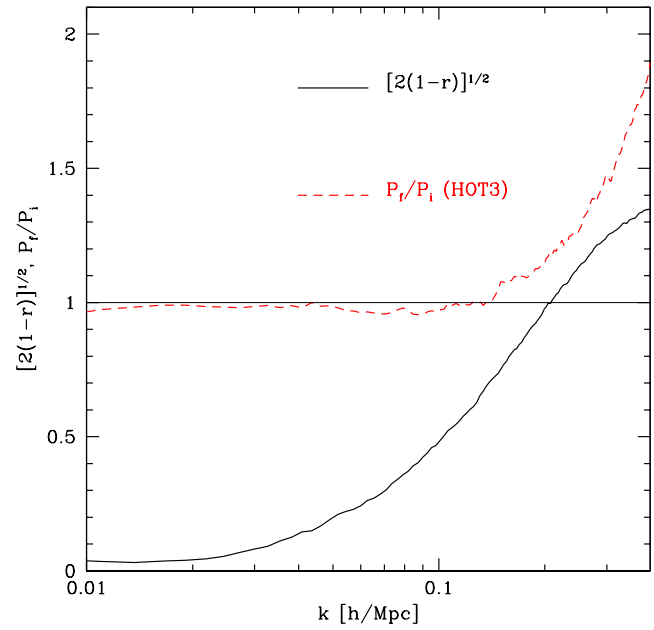


Figure 2. Relative rms fluctuation $\sigma_b/b = [2(1 - r)]^{1/2}$ between the final and the initial density field for HOT3 (solid). Also shown is the power spectrum ratio between the two fields (dashed). Results for HOT2 are very similar.

We can define the ratio of the power spectra as

$$\langle b^2(k) \rangle \equiv \frac{P_f(k)}{P_i(k)} = \frac{\langle \delta_f^2(\mathbf{k}) \rangle}{\langle \delta_i^2(\mathbf{k}) \rangle}, \quad (1)$$

where $\langle \rangle$ denotes ensemble average over different realizations of the universe. We can define relative rms fluctuations in b as

$$\left(\frac{\sigma_b}{b} \right)^2 = \frac{\langle (\delta_f - \langle b^2 \rangle^{1/2} \delta_i)^2 \rangle}{\langle \delta_f^2 \rangle}. \quad (2)$$

This is related to the cross-correlation coefficient r , defined as

$$r(k) = \frac{\langle \delta_i(\mathbf{k}) \delta_f(\mathbf{k}) \rangle}{\sqrt{\langle \delta_i(\mathbf{k}) \delta_i(\mathbf{k}) \rangle \langle \delta_f(\mathbf{k}) \delta_f(\mathbf{k}) \rangle}}. \quad (3)$$

The two are related via

$$\frac{\sigma_b}{b} = \sqrt{2(1 - r)}. \quad (4)$$

Figure 2 shows σ_b/b as a function of wavemode k , where the average has been done over a large number of wavemodes so that r converges (at very low k this condition is not satisfied and r is biased high, which underestimates the rms fluctuations). We see that σ_b/b changes from 10% at $k \sim 0.02h/\text{Mpc}$ to 40% at $0.1h/\text{Mpc}$, above which it rapidly increases and the two fields become incoherent. Figure 2 also shows the ratio of nonlinear to linear power spectrum at $z = 0$, $\langle b^2(k) \rangle$. For $k > 0.15h/\text{Mpc}$ the final power spectrum rapidly grows with k and exceeds the linear power spectrum, while for $k < 0.15h/\text{Mpc}$ the final spectrum is slightly anti-biased on large scales, ie $P_f(k) < P_i(k)$.

The main result arising from figures 1-2 is that the fluctuations between the linear and nonlinear fields are large on

large scales, despite the fact that the nonlinear power spectrum is very close to the linear one. This is not so evident from the cross-correlation coefficient r itself, which can be close to 1 and still lead to large rms fluctuations: even for $r = 0.995$ the fluctuations between initial and final field are 10% for any given mode.

One can get some understanding of these results by using second order perturbation theory results (see Bernardeau et al. 2002, for a recent review). To compute the power spectrum to second order one must derive the density field to 3rd order, $\delta = \delta_1 + \delta_2 + \delta_3$. Second order contributions to the power spectrum arise both from $\delta_2\delta_2$ and $\delta_1\delta_3$ terms. The $\delta_2\delta_2$ is the mode-mode coupling term, while the $\delta_1\delta_3$ is the nonlinear growth evolution term. These terms have different behaviour in various limits and have differing signs in the contribution: while $\delta_2\delta_2$ is strictly positive, $\delta_1\delta_3$ has a negative component. For $k < 0.15h/\text{Mpc}$ the negative contribution wins and the second order correction to the power spectrum is negative. At its peak around $k \sim 0.1h/\text{Mpc}$ the correction is 5% and slowly decreases towards $k \rightarrow 0$. While the correction is small on average, this is a result of a cancellation between positive and negative contributions. The dominant perturbative corrections come from the modes close to the mode itself: for $k = 0.1/\text{Mpc}$ the dominant contribution to the positive component is from the modes around $k \sim 0.05/\text{Mpc}$, which contribute around a third of the total correction or around 5% of the final power spectrum (Jain & Bertschinger 1994). These are long wavelength modes and in any finite volume there will be large statistical fluctuations in their power relative to the true power. This leads to significant fluctuations in the second order corrections depending on the actual realization of the mode amplitudes. Thus the final amplitudes of individual modes fluctuate significantly relative to their initial values because of perturbative large scale effects.

4 STOCHASTICITY OF HALOS

Galaxies are believed to form inside dark matter halos, which are virialized structures of high density. They can be labelled by their virial mass. Observations suggest that about 80% of the galaxies in a typical flux limited survey form at the centers of halos with masses ranging between $10^{11}h^{-1}M_{\odot}$ to $10^{13}h^{-1}M_{\odot}$, while the remaining 20% of galaxies are non-central and occupy groups and clusters (Guzik & Seljak 2002). The exact radial distribution of galaxies inside halos and the form of the halo mass probability distribution is the subject of a lot of current observational and theoretical effort. Here we will use centers of dark matter halos as a proxy for galaxy positions. This will not give the correct correlation properties on small scales, where correlations between central and noncentral galaxies within the halos are important, but should be valid on large scales, where halos can be thought of as pointlike. We will show the results for a range of halo masses, which can be roughly thought as corresponding to galaxies with different luminosities since there is a tight relation between the halo mass and luminosity (McKay et al. 2001; Guzik & Seljak 2002). Alternatively, the different samples can be thought of as varying the flux limit of a survey, since going to fainter limits increases the number density of galaxies and thus reduces the

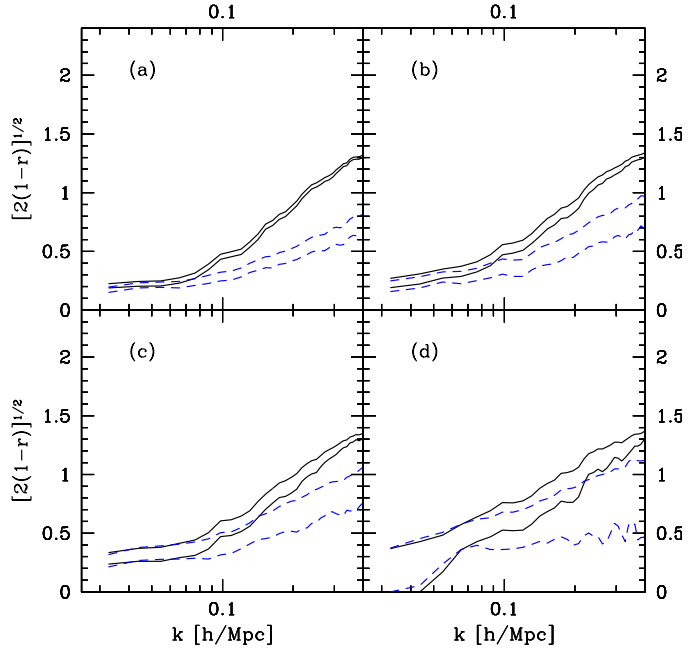


Figure 3. Relative rms fluctuation $\sigma_b/b = \sqrt{2(1-r)}$ between the halo density field and the initial (solid) or final (dashed) matter density field. Lower curves have been obtained by applying the shot noise subtraction from the halo power spectrum. Average masses are $4.5 \times 10^{11}h^{-1}M_{\odot}$ (a), $10^{12}h^{-1}M_{\odot}$ (b), $2 \times 10^{12}h^{-1}M_{\odot}$ (c) and $10^{13}h^{-1}M_{\odot}$ (d). The corresponding halo densities are $7 \times 10^{-3}h^3/\text{Mpc}^3$, $2.7 \times 10^{-3}h^3/\text{Mpc}^3$, $1.5 \times 10^{-3}h^3/\text{Mpc}^3$ and $3.5 \times 10^{-4}h^3/\text{Mpc}^3$.

shot noise and the same effect is achieved by going to fainter galaxies.

Dark matter halos are identified from the simulations using the standard friends of friends algorithm with a linking length of 0.2. The resulting mass functions agree well with the fitting formulae in the literature (Sheth & Tormen 1999; Jenkins et al. 2001). We order them by mass and use subsamples separated roughly by a factor of 2 in mass. As in previous section we can define the halo fluctuation $\delta_h(\mathbf{k})$ and bias $b(\mathbf{k}) = \delta_h(\mathbf{k})/\delta_m(\mathbf{k})$, as well as the cross-correlation coefficient between the two fields (equation 3). Figure 3 shows the relative rms fluctuations σ_b/b as a function of scale for several halo masses, relative to both the initial and the final density field. We show the case with and without the subtraction of shot noise contribution to the halo power spectrum (the dark matter power spectrum does not require shot noise subtraction because of large number of dark matter particles). The lines without shot noise subtraction are always above the ones with subtraction and are the relevant ones if one is interested in the stochasticity between the halos and dark matter. The lower lines for which the shot noise has been subtracted show the remaining stochasticity which is not due to the shot noise. Because of the shot noise subtraction the cross-correlation coefficient can exceed 1, in which case we do not show the result.

From figure 3 we see that the halos are even less well correlated to the initial density field than the dark matter is. The stochasticity begins at the level of 20% at low k , increasing to 50% at $k \sim 0.1h/\text{Mpc}$. The shot noise contribution

to stochasticity is small for halos with high spatial density (low mass halos), but increases significantly for halos with low spatial density, as expected. There is no obvious difference in the shot noise subtracted values, suggesting that the shot noise simply adds an additional component of stochasticity on top of that induced by nonlinearities in the relation between the halos and the initial density field.

Correlation coefficient between the halos and the final density field is also shown in figure 3 (dashed lines). Compared to the halo-initial field correlations the stochasticity is similar on the largest scales, but there is a better agreement between the halo and the final dark matter field on smaller scales ($k > 0.1h/\text{Mpc}$). The cross-correlation coefficient r would likely be even larger on small scales if we had modelled the galaxy distributions within the halos more realistically, since this would lead to an enhancement of correlations on small scales, similar to that seen in the dark matter. Results from GIF simulations and analytic results using halo models suggest that the cross-correlation coefficient can remain close to unity up to a fairly high $k \sim 1h/\text{Mpc}$ (Seljak 2000), but this may not be generic and depends on the details of how galaxies are populated within the halos, which are quite uncertain. Observational evidence suggests that there is some stochasticity on 1Mpc scale, with $r \sim 0.5$ (Hoekstra et al. 2002). If $r < 1$ it would complicate the interpretation of the results based on the comparison between galaxy-galaxy correlations and galaxy-dark matter correlations, such as those from the galaxy-galaxy lensing analysis (Sheldon et al. 2003). Here we are more concerned with the correlations on large scales, $k < 0.1h/\text{Mpc}$, where the details of galaxy distribution within halos are not important and where direct observations are not yet available. The results suggest that the fluctuations between halos and initial or final matter field are never below 10-20%.

The dark matter distribution cannot be directly observed, so results shown in figure 3 are not directly applicable to any observational test. The closest example to a direct observation of the dark matter is through the weak lensing effect. Here the light from distant galactic sources is being distorted by the mass distribution along the line of sight. By averaging over the image distortions we can reconstruct the 2-d shear and convergence maps. These are given by the line of sight projection of the matter density, weighted by a radial function that is very broad. Correlations at a given angular scale receive dominant contributions from a transverse distance at half the distance to the source, but significant contributions are also coming from much smaller transverse separations produced by the mass distribution closer to the observer.

It has been suggested by Pen (2004) that if one cross-correlates the properly radially weighted galaxy field with the weak lensing maps then one determines the bias of galaxies exactly if the two are perfectly correlated. Under these assumptions one can use the galaxy clustering information to determine the amplitude of dark matter fluctuations with higher accuracy than from the weak lensing itself, because the galaxy clustering can be done in 3-d (if redshifts are measured) and so one has more independent modes to reduce the sampling variance compared to the 2-d analysis. For this method to work the correlation between the projected matter density and galaxy field must be close to perfect.

To address this assumption one must correlate 2-d pro-

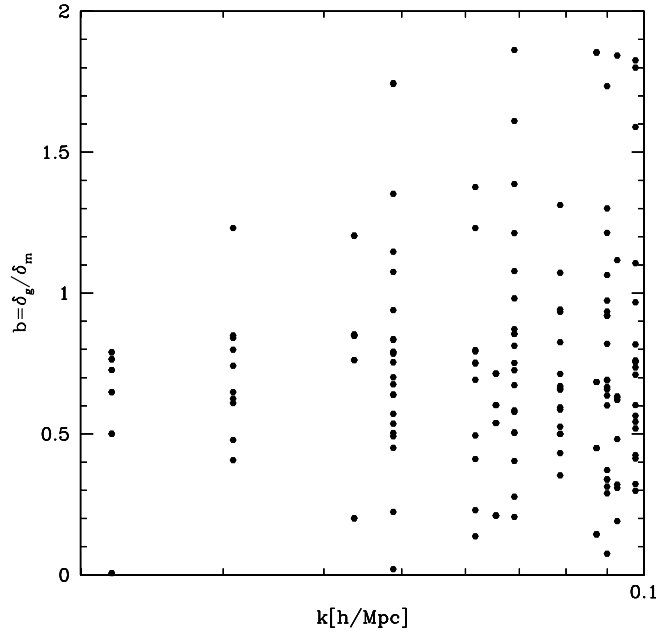


Figure 4. Ratio of 2-d projected halo density perturbations ($M = 10^{11}h^{-1}M_{\odot}$) to the initial density field as a function of wavemode amplitude k . The projections are along each of the three axes ($288h^{-1}\text{Mpc}$ for HOT2 simulation used here). The scatter is larger than the corresponding 3-d case in figure 3.

jections of final dark matter and galaxies. While properly projected weak lensing 2-d maps have been constructed from N-body simulations (Jain et al. 2000; White & Hu 2000), we take a simplifying approach here and cross-correlate the 2-d projections of the simulations along each of the 3 axes. The resulting rms scatter as a function of projected wavevector k is found to be significantly larger than in 3-d case, a consequence of the projection effects, which cause shorter wavelength modes to contribute to longer wavelength modes in projection. For $10^{12}h^{-1}M_{\odot}$ halos, which corresponds roughly to L_* galaxies, we find that the rms scatter is 20% at $k \sim 0.03h/\text{Mpc}$ and 40% at $k \sim 0.1h/\text{Mpc}$. This is reduced by a factor of 2 if $10^{11}h^{-1}M_{\odot}$ galaxies are used instead. This last example is shown in figure 4. In reality the stochasticity is likely to be larger for the lensing case, since projections at a fixed angle (rather than at a fixed transverse separation as done here) receive contributions from nearby small scale structures, for which the stochasticity between the galaxies and the dark matter will be much larger.

We can estimate the effect of this scatter on the amplitude determination from the weak lensing cross-correlation analysis. If the lensing kernel peaks at $z \sim 0.3 - 0.4$ then $k \sim 0.1h/\text{Mpc}$ corresponds to $l \sim 100$. In a 200 square degree survey such as the upcoming CFHT Legacy Survey (Van Waerbeke & Mellier 2003) we will have about 5 independent modes at $l \sim 30$ and 50 at $l \sim 100$. This means that for galaxies in $10^{12}h^{-1}M_{\odot}$ halos the overall linear amplitude will have an error of $20\%/\sqrt{5} \sim 9\%$ at $l \sim 30$ and 6% at $l \sim 100$, arising just from this effect (the power spectrum amplitude error will be twice as large). Additional errors of comparable magnitude will arise from the lensing noise and projection effects. Such a poor determination of the growth

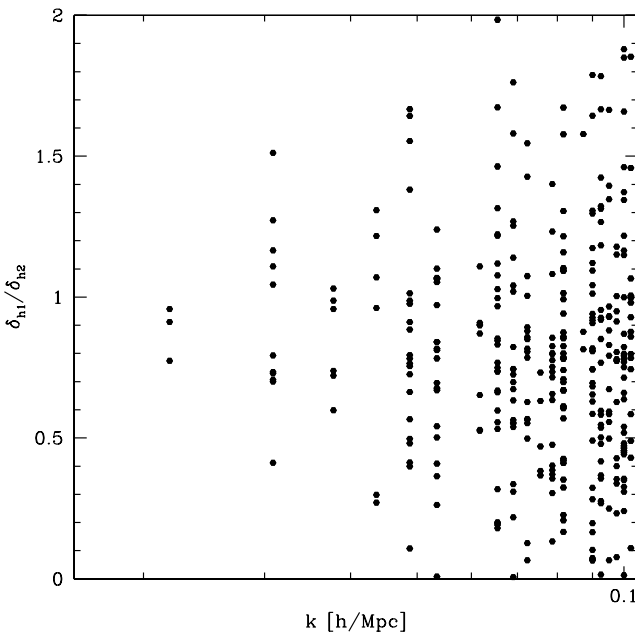


Figure 5. Ratio of halo density perturbations δ_{h1}/δ_{h2} as a function of wavemode amplitude k . The halos are of mass $10^{11}h^{-1}M_{\odot}$ (h1) and $10^{12}h^{-1}M_{\odot}$ (h2).

factor as a function of redshift is unlikely to improve our current constraints on the dark energy significantly. This source of error was not included in the previous analysis (Pen 2004) and is much larger than the prognosticated errors without it. This complicates the prospects of this method for studies of dark energy through the growth factor evolution. The errors can be reduced with a larger survey area: for a survey covering 25% of full sky the errors on the power spectrum amplitude may approach 1% because more modes are being sampled and because the largest modes have the smallest amount of stochasticity. It remains to be seen whether this is ever competitive with a straight weak lensing analysis on smaller scales.

As discussed in the introduction another method to determine the bias is to combine the clustering analysis of faint galaxies, for which we know the theoretical bias, with the luminous galaxies, for which we can measure the clustering on large scales with a small statistical error. To determine the relative bias between the populations we can simply compare the smoothed maps. In the absence of stochasticity between the two galaxy populations one could determine the amplitude of mass fluctuations directly. Suppose that we want to determine the clustering amplitude of faint galaxies, which are in low mass halos (around $10^{11}h^{-1}M_{\odot}$ for galaxies 2-3 magnitudes below L_*) and L_* galaxies, which typically occupy $10^{12}h^{-1}M_{\odot}$. Figure 5 shows the relative rms fluctuations in ratios of Fourier mode amplitudes between halos of mass $10^{11}h^{-1}M_{\odot}$ and $10^{12}h^{-1}M_{\odot}$. We see again from figure 5 that the scatter is large. Both shot noise and stochasticity due to nonlinearities limit this method. The rms fluctuations between $10^{11}h^{-1}M_{\odot}$ and $10^{12}h^{-1}M_{\odot}$ halos are 8% at $k \sim 0.1h/\text{Mpc}$ and 23% at $k \sim 0.2h/\text{Mpc}$. This is somewhat smaller than between the halos and the matter. Moreover, galaxies in redshift surveys provide 3-d

information, so there are more large scale modes to reduce the scatter. Nevertheless, any attempt to determine the linear bias using the cross-correlations must include this source of stochasticity in the analysis.

5 HALO BIAS AS A FUNCTION OF MASS

One of the important questions that can be addressed with these simulations is the relation between halo and dark matter power spectrum as a function of halo mass. This relation has been theoretically predicted from the spherical collapse model (Cole & Kaiser 1989; Mo & White 1996) and from the ellipsoidal collapse model (Sheth et al. 2001), which suggest that the halo bias is related to a derivative of the halo mass function. The relation has also been extracted from the numerical simulations, with a good quantitative agreement between the theoretical predictions and the simulations over a range of different cosmological models (Jing 1998; Sheth & Tormen 1999). Since these comparisons were done for a wide range of initial power spectra they were not specifically designed for realistic Λ CDM models and the predictions and simulations could differ by up to 20%. Moreover, the simulations used in previous work were based on 256^3 particle simulations and did not have sufficient dynamic range to sample the long wavelength modes and resolve small halos at the same time. For the more massive halos shot noise is large, so the bias estimate is noisy. For halos close to the resolution threshold (typically of the order of 50-100 particles) some fraction of the halos may be missed by the halo finder, leading to biased results in the bias determination as the low mass end.

The simulations used in this paper are a significant improvement over the previous generation. They contain 8-27 times more particles and cover a wide range of masses. We use HOT1 simulation for halos in the mass range $(5 \times 10^{10} - 3 \times 10^{11})M_{\odot}$, HOT2 for halos in the mass range $(3 \times 10^{11} - 10^{14})M_{\odot}$ and HOT3 for halos in the mass range $(10^{13} - 10^{15})M_{\odot}$.

Figure 6 shows the ratio of the (shot noise corrected) halo power spectrum to the linear mass power spectrum as a function of a wavevector k . One can see that the assumption of constant bias is reasonable for $k < 0.1h/\text{Mpc}$ and even beyond, so a linear bias can be defined as an appropriate average over these modes. The exception are the most massive halos in HOT3 with $b > 1.5$, for which the power spectrum is suppressed already at $k \sim 0.1h/\text{Mpc}$ due to the fact that the FOF halos do not overlap and so cannot be closer than two times the virial radius. Here we use all of the modes with $k < 0.1h/\text{Mpc}$, except for the smallest $96h^{-1}\text{Mpc}$ simulation where we use $k < 0.15h/\text{Mpc}$. We note that there is a good agreement between the simulations in the overlap mass range, but the larger simulation has smaller statistical errors. The smallest simulation (HOT1) has very few modes in the linear regime and the fluctuations in the ratio caused by perturbative effects beyond linear theory are large, so the bias determination from this simulation is somewhat less reliable. On the other hand, all of the low mass halos in this simulation have almost the same bias and at the upper end of the mass range there is a good agreement in bias with halos of the same mass from HOT2.

For simplification with theoretical comparisons we will

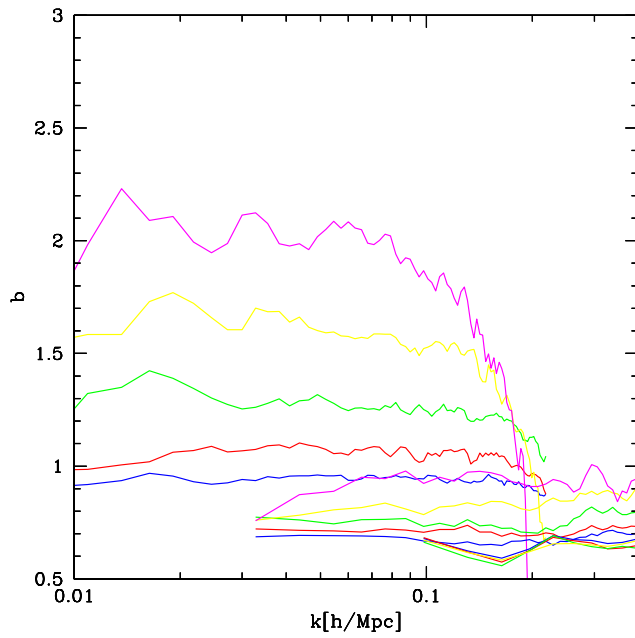


Figure 6. Ratio of halo to linear density field power spectrum as a function of wavevector k for halos of varying mass. At the bottom are the halos from HOT1 simulation, next up are those from HOT2 and at the top are the HOT3 halos.

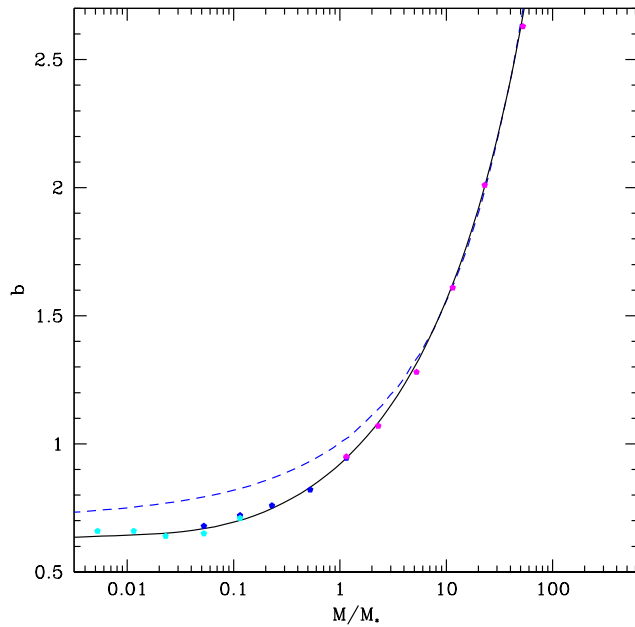


Figure 7. Bias as a function of mass in units of the nonlinear mass. Points are from HOT1 (lowest masses), HOT2 (intermediate masses) and HOT3 (highest masses) simulations. We only show HOT1-3, but we have several other simulations of this model which agree with these results. Note that in a few cases the points from two simulations overlap exactly. Upper (dashed blue) line is theoretical prediction from Sheth and Tormen (1999). Lower (solid black) line is the expression from equation 5.

scale all the masses relative to the nonlinear mass M_{nl} , defined as the mass within a sphere for which the rms fluctuation amplitude of the linear field is 1.68. While the theoretical predictions for the bias depend on the cosmological model, most of that dependence is accounted for if the mass is expressed in terms of the nonlinear mass. For HOT1-3 simulations with $\sigma_8 = 0.9$ and $\Omega_m = 0.3$ at $z = 0$ the nonlinear mass is $8.75 \times 10^{12} h^{-1} M_\odot$. Figure 7 shows the bias determinations as a function of halo mass from the simulations used in this paper. The dashed line is the theoretical prediction from Sheth & Tormen (1999) (the fitting formula given in Jing (1998) is very similar; while these fitting formulae are not very accurate we find a good agreement between the simulation results in these papers and our simulations). We see that these theoretical predictions overestimate the bias below M_{nl} and are a good fit above M_{nl} . The largest discrepancy is below M_{nl} , where the relative error can be up to 20%. The various simulations are in a reasonable agreement among themselves and the scatter between the points at the same mass is mostly due to the shot noise and small volume over which one is averaging. There may be some systematical error due to the fact that the nonlinear mass computed from the theoretical power spectrum can differ from the value obtained if one uses the actual realization. We find this can lead up to a 10% effect on nonlinear mass and would cause a horizontal shift by this amount. This is of almost no consequence for masses below M_{nl} , where bias is only weakly dependent on the mass, but may lead to a larger error at the high mass end.

We find that the unbiased galaxies with $b = 1$ are at $M = 1.5 M_{\text{nl}}$ and the bias is rapidly changing above $0.1 M_{\text{nl}}$, while below this it is essentially constant with the value around 0.65. In all simulations we see a hint of bias increasing at the lowest masses (figure 8), but it is likely that this is a numerical artifact, since a similar increase is also seen in HOT2 at the low mass end and is not confirmed in HOT1, where the mass resolution improves by a factor of 8 (figure 8). With another $96 h^{-1} \text{Mpc}$ box 512^3 particle simulation we have verified that $b \sim 0.65$ at the low mass end is consistent and not a result of sampling error in HOT1.

The solid curve in figure 7 is an empirical expression that fits HOT1-3 simulations. Over the range between $10^{-3} < M/M_{\text{nl}} < 10^2$ it is given by

$$b_0(x = M/M_{\text{nl}}) = 0.53 + 0.39x^{0.42} + \frac{0.08}{40x + 1} + 10^{-4}x^{1.7}. \quad (5)$$

This expression should be accurate to about 3% or better for this model (figure 7).

In figure 8 we show the bias as a function of mass for several simulations for which we varied one parameter at a time, roughly spanning the range of interest from cosmological constraints today. We see that there is very little difference in the theoretical predictions for halo bias as a function of M/M_{nl} , suggesting that instead of deriving full expressions, which depend on all cosmological parameters, one can simply use a single relation with mass in units of nonlinear mass, as in equation 5. The deviations from this relation are qualitatively consistent with the predictions given by Sheth & Tormen (1999). We can generalize the results from equation 5 by linearizing the bias relation in terms of

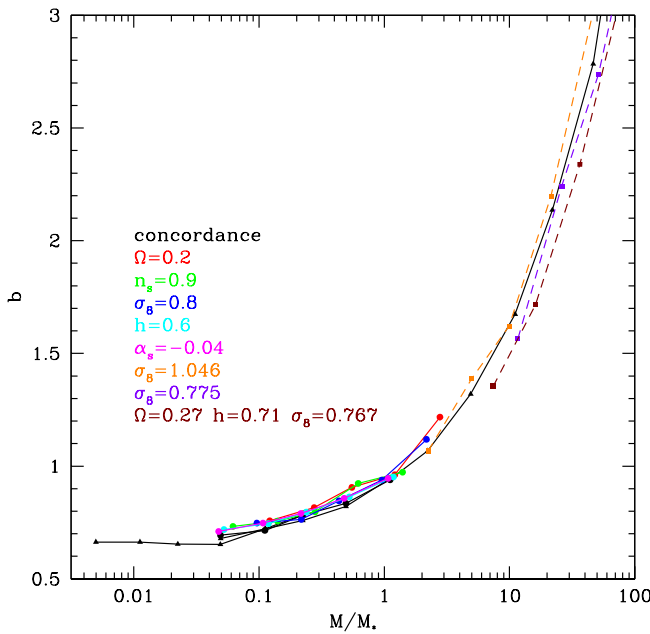


Figure 8. Bias as a function of mass in units of the nonlinear mass for several cosmological models. We varied one parameter at a time relative to the fiducial concordance model, roughly covering the range of interest. This figure shows that the bias predictions depend predominantly on the nonlinear mass, while other cosmological parameters play only a minor role.

cosmological parameters,

$$b(x) = b_0(x) + \log_{10}(x)[0.4(\Omega_m - 0.3 + n_s - 1) + 0.3(\sigma_8 - 0.9 + h - 0.7) + 0.8\alpha_s]. \quad (6)$$

This correction should be reasonable for $x > 0.1$, while below that one should have a constant correction $-0.4[\Omega_m - 0.2 + n_s - 1] - 0.3[\sigma_8 - 0.9 + h - 0.7] - 0.8\alpha_s$. For massive halos with $M > M_{\text{nl}}$ the differences among models in the bias predictions from Sheth & Tormen (1999) become larger, but this is difficult to observe in these simulations, where the number of such halos is small and the bias measurements have large shot noise. In this regime the analytic predictions may be more accurate than equation 5. Note however that for the fiducial model the two agree very well and that the simulations used in this paper improve upon the previous generation simulations over this regime as well.

6 CONCLUSIONS

In this paper we have addressed the relations between the matter density field, halos and initial density field, focusing on large scales where these are often assumed to be proportional to each other. We focus on two issues. First, what is the scatter between these fields around the average relation? This is expressed here in terms of relative scatter between the amplitudes of fluctuations, which is related to the stochasticity parameter r , defined as the cross-correlation coefficient between the two fields. Even small deviations of r from unity give large relative fluctuations between the two fields. These are of interest whenever one is trying to relate

the fields to one another to determine their relative amplitudes. One example is the bias determination using the cross-correlation between the weak lensing signal (tracing the matter density) and the galaxies. Another example is the relative bias determination between two different galaxy populations, which we propose here as an alternative method to determine the galaxy bias, because galaxies in low mass halos have a bias of $b \sim 0.7$ independent of their mass. In all cases we find the scatter between the fields in individual modes is significant and one cannot assume the fields are simply proportional one to another. This scatter, coupled with a small number of modes on large scales, makes it difficult to accurately determine the bias (or relative bias) and needs to be included in the predictions of how accurately one can determine the matter power spectrum with these methods.

The second goal of this paper was to revisit the halo bias as a function of halo mass. This relation is a fundamental ingredient of any halo model (see Cooray & Sheth 2002, for a recent review) and plays an important role if one is trying to model galaxy clustering by connecting it to the underlying halos. The previous generation of simulations (Jing 1998; Sheth & Tormen 1999) had a limited dynamical range and the predictions were not tuned specifically for Λ CDM models. As a result the existing expressions overestimate the bias by as much as 20% in the range below the nonlinear mass, which is likely to be the mass range for halos that host most of the galaxies. We propose a new expression that fits the simulations better. We argue that this expression should be fairly accurate for other cosmological models of interest as well, as long as the mass is expressed in units of nonlinear mass and give corrections for small deviations from this model. The overall accuracy on bias-halo mass relation is at the level of 0.03 or better (for $b < 1$), which should help with the bias determination from the current generation of observations.

We thank P. McDonald, N. Padmanabhan and L. Teodoro for help and useful comments, and S. Habib for encouraging this collaboration. US is supported by Packard Foundation, Sloan Foundation, NASA NAG5-1993 and NSF CAREER-0132953. Simulations by MSW were performed on the Space Simulator Beowulf Cluster and ASCI Q at Los Alamos. Work by MSW was performed under the auspices of the U.S. Dept. of Energy, and supported by its contract #W-7405-ENG-36 to Los Alamos National Laboratory.

REFERENCES

- Bernardeau F., Colombi S., Gaztanaga E., Scoccimarro R., 2002, Phys. Rep., 367, 1
- Cole S., Kaiser N., 1989, MNRAS, 237, 1127
- Cooray A., Sheth R., 2002, Phys. Rep., 372, 1
- Frenk C. S. et al., 1999, ApJ, 525, 554
- Guzik J., Seljak U., 2002, MNRAS, 335, 311
- Hoekstra H., van Waerbeke L., Gladders M. D., Mellier Y., Yee H. K. C., 2002, ApJ, 577, 604
- Jain B., Bertschinger E., 1994, ApJ, 431, 495
- Jain B., Seljak U., White S., 2000, ApJ, 530, 547
- Jenkins A., Frenk C. S., White S. D. M., Colberg J. M., Cole S., Evrard A. E., Couchman H. M. P., Yoshida N., 2001, MNRAS, 321, 372

Jing Y. P., 1998, *ApJ*, 503, L9
 Matsubara T., 1999, *ApJ*, 525, 543
 McKay T. A. et al., 2001, in *astro-ph/0108013*
 Mo H. J., White S. D. M., 1996, *MNRAS*, 282, 347
 Pen U., 2004, ArXiv Astrophysics e-prints
 Percival W. J. et al., 2002, *MNRAS*, 337, 1068
 Salmon J. K., Warren M. S., 1994, *J. Comp. Phys.*, 111, 136
 Seljak U., 2000, *MNRAS*, 318, 203
 Seljak U., Zaldarriaga M., 1996, *ApJ*, 469, 437
 Sheldon E. S. et al., 2003
 Sheth R. K., Mo H. J., Tormen G., 2001, *MNRAS*, 323, 1
 Sheth R. K., Tormen G., 1999, *MNRAS*, 308, 119
 Tegmark M. et al., 2003, ArXiv e-print *astro-ph/0310725*
 Van Waerbeke L., Mellier Y., 2003, ArXiv Astrophysics e-prints
 Warren M. S., Salmon J. K., 1993, in *Supercomputing '93*.
 IEEE Comp. Soc., Los Alamitos
 White M., Hu W., 2000, *ApJ*, 537, 1